A single residue in Ebola virus receptor NPC1 influences cellular host range in reptiles

Esther Ndungo[1], Andrew S. Herbert[2], Matthijs Raaben[3,4], Gregor Obernosterer[4], Rohan Biswas[1], Emily Happy Miller[1], Ariel S. Wirchnianski[2], Jan E. Carette[5], Thijn R. Brummelkamp[4], Sean P. Whelan[3], John M. Dye[2a], and Kartik Chandran[1a]

[1]Department of Microbiology and Immunology, Albert Einstein College of Medicine, 1300 Morris Park Ave, Bronx, NY 10461, USA;

[2]United States Army Medical Research Institute of Infectious Diseases, 1425 Porter St, Fort Detrick, MD 21702-5011, USA;

[3]Department of Microbiology and Immunobiology, 200 Longwood Ave, Harvard Medical School, Boston, MA 02115, USA;

[4]Netherlands Cancer Institute, Plesmanlaan 121, 1066 CX Amsterdam, The Netherlands.

[5]Department of Microbiology and Immunology, Stanford University School of Medicine, 299 Campus Drive, Stanford, CA 94305, USA.

[a]Corresponding authors. Kartik Chandran#, email: kartik.chandran@einstein.yu.edu

John M. Dye#, email: john.m.dye1.civ@mail.mil

Running title: Ebola virus host range determinants in reptiles

Abstract word count: 244

Text word count: 4280

Abstract

Filoviruses are the causative agents of an increasing number of disease outbreaks in human populations, including the current unprecedented Ebola virus disease (EVD) outbreak in Western Africa. One obstacle to controlling these epidemics is our poor understanding of the host range of filoviruses and their natural reservoirs. Here, we investigated the role of the intracellular filovirus receptor, Niemann-Pick C1 (NPC1) as a molecular determinant of Ebola virus (EBOV) host range at the cellular level. Whereas human cells can be infected by EBOV, a cell line derived from a Russell's viper (*Daboia russellii*) (VH-2) is resistant to infection in an NPC1-dependent manner. We found that VH-2 cells are resistant to EBOV infection because the Russell's viper NPC1 ortholog bound poorly to the EBOV spike glycoprotein (GP). Analysis of panels of viper-human NPC1 chimeras and point mutants allowed us to identify a single amino acid residue in NPC1, at position 503, that bidirectionally influenced both its binding to EBOV GP as well as its viral receptor activity in cells. Significantly, this single residue change perturbed neither NPC1's endosomal localization nor its housekeeping role in cellular cholesterol trafficking. Together with other recent work, these findings identify sequences in NPC1 that are important for viral receptor activity by virtue of their direct interaction with EBOV GP, and suggest that they may influence filovirus host range in nature. Broader surveys of *NPC1* orthologs from vertebrates may delineate additional sequence polymorphisms in this gene that control susceptibility to filovirus infection.

Importance

Identifying cellular factors that determine susceptibility to infection can help us understand how Ebola virus is transmitted. We asked if the EBOV receptor, Niemann-Pick C1 (NPC1) could ex-

plain why reptiles are resistant to EBOV infection. We demonstrate that cells derived from the Russell's viper are not susceptible to infection because EBOV cannot bind to viper NPC1. This resistance to infection can be mapped to a single amino acid residue in viper NPC1 that renders it unable to bind to EBOV GP. The newly solved structure of EBOV GP bound to NPC1 confirms our findings, revealing that this residue dips into the GP receptor-binding pocket, and is therefore critical to the binding interface. Consequently, this otherwise well conserved residue in vertebrate species influences the ability of reptilian NPC1s to bind to EBOV GP, thus affecting cellular host range.

Introduction

Ebola virus (EBOV) is the causative agent of highly lethal zoonotic infections in humans and non-human primates in sub-Saharan Africa (1-3). Despite the emerging roles of EBOV and related members of the family *Filoviridae* (filoviruses) in human disease, our knowledge of the ecologic host range of these agents remains limited. Bats are thought to be important reservoirs for filoviruses; however, conclusive evidence in favor of this hypothesis has been obtained only for Marburg virus (MARV) and Ravn virus (RAVV), which were recently found to circulate in Egyptian rousettes (*Roussetus aegyptiacus*) (4-7).

Previous studies demonstrated that, whereas a broad range of mammalian and avian cell lines are susceptible to EBOV and/or MARV, all tested reptilian and amphibian lines are resistant to infection (8-10). These findings suggested the existence of one or more unknown determinants of filovirus host range. Although the determinants of filovirus infection and disease at the organismal level are likely to be complex, it is well established that interactions between viruses and cell-intrinsic host factors, such as entry receptors, can dictate host range. For example, ortholog-specific sequence variations in angiotensin-converting enzyme 2 (ACE2) and transfer-

rin receptor (TfR1) influence the host range of viruses for which they serve as receptors (severe acute respiratory syndrome-related coronaviruses (11, 12); New World mammarenaviruses, canine parvoviruses, and murine mammary tumor virus (13-18), respectively). Jae and co-workers demonstrated that chicken cells are resistant to infection by an Old World arenavirus, Lassa virus, because of a single amino acid difference in the chicken ortholog of its intracellular receptor, LAMP1 (19).

We and others recently demonstrated that Niemann-Pick C1 (NPC1), a large endo/lysosomal membrane protein involved in cellular cholesterol trafficking, is an essential intracellular receptor for filovirus entry and infection (20-23). We also found that NPC1 could influence the cellular host range of filoviruses–human NPC1 conferred susceptibility to filovirus entry and infection when expressed in the non-permissive reptilian cell line VH-2, derived from a Russell's viper (*Daboia russellii*) (22). In that study, however, we did not establish the molecular basis of the NPC1-dependent block to viral entry in VH-2 cells.

Recently, we found that a single amino acid residue (502) in the second luminal domain of NPC1, domain C, is under positive selection in bats, and controls susceptibility of bat cells to EBOV infection in a host species-dependent manner (24). Here, we demonstrate that an adjacent residue, 503, highly conserved in the domain C of NPC1, also influences EBOV host range in reptilian cells by controlling its activity as a filovirus receptor. The recently solved structure of EBOV GP bound to domain C shows that these two residues are in a loop that dips into the exposed receptor-binding site (25). Therefore, our findings identify a hotspot in NPC1 at the EBOV GP-binding interface that influences virus-receptor recognition and host cell susceptibility, suggesting evolutionary scenarios in which antagonism with filoviruses could sculpt host *NPC1* genes selectively, without compromising their ancient, and essential, function in cellular choles-

terol homeostasis.

Results

The second luminal domain of the Russell's viper NPC1 ortholog binds poorly to the Ebola virus glycoprotein. We postulated that EBOV fails to enter and infect Russell's viper VH-2 cells because the EBOV entry glycoprotein, GP, cannot recognize the viper ortholog of the filovirus intracellular receptor, Niemann-Pick C1 (*Dr*NPC1). We previously showed that the second luminal domain (C) of human NPC1 (*Hs*NPC1) directly contacts a cleaved form of EBOV GP (GP_{CL}), and that GP_{CL}–*Hs*NPC1 domain C binding is essential for filovirus entry (22, 23). Accordingly, we investigated the capacity of *Dr*NPC1 domain C to bind to GP_{CL} and support EBOV entry and infection.

We first used reverse-transcription PCR (RT-PCR) to isolate and sequence the *Dr*NPC1 domain C gene. Alignment of domain C amino acid sequences from *Hs*NPC1 and *Dr*NPC1 revealed a substantial degree of conservation (80% amino acid identity), with identical arrangements of cysteine residues and similar predicted secondary structures, suggesting a similar overall fold for both proteins (Fig. 1).

To facilitate *in vitro* GP_{CL}–NPC1 binding studies, we engineered a soluble form of *Dr*NPC1 domain C, as previously described for *Hs*NPC1 (22). Transfection of HEK 293T cells with this construct afforded the secretion of an extensively *N*–glycosylated form of *Dr*NPC1 domain C (Fig. 2A). As shown previously, purified *Hs*NPC1 domain C could bind to recombinant vesicular stomatitis Indiana virus particles bearing cleaved EBOV GP (rVSV-GP_{CL}) as measured by ELISA(22); however, no ELISA signal was apparent even at the highest concentration of *Dr*NPC1 domain C (Fig. 2B). Therefore, *Dr*NPC1 domain C, in contrast to its human

counterpart, recognizes the EBOV glycoprotein poorly or not at all.

***Dr*NPC1 domain C can substitute for *Hs*NPC1 domain C in mediating endo/lysosomal cholesterol clearance but not EBOV entry and infection.** While the efficient secretion of the soluble, glycosylated *Dr*NPC1 domain C construct suggested that it was not misfolded, it was nevertheless conceivable that subtle structural aberrations rendered this protein biologically inactive. Accordingly, we assessed the capacity of *Dr*NPC1 domain C to support NPC1's best-established cellular function—clearance of unesterified cholesterol from endo/lysosomal compartments (Fig. 3A-B). This activity requires the full-length NPC1 protein, including all three major luminal domains, A, C, and I. We therefore generated and tested an *Hs*NPC1 chimera in which domain C (residues 373–620) was seamlessly replaced with its viper counterpart (*Hs*NPC1–*Dr*C), and stably expressed this construct in the NPC1-null Chinese hamster ovary (CHO) M12 cell line (26). As expected, immunostaining of NPC1 in a stable cell line expressing WT *Hs*NPC1 revealed a punctate, predominantly perinuclear distribution and 'donut-like' structure characteristic of NPC1's localization to the limiting membrane of late endosomes and lysosomes (Fig. 3A). This distribution could be readily contrasted with the filigree-like pattern obtained with *Hs*NPC1(I1061T), a point mutant that is susceptible to misfolding and is largely retained in the endoplasmic reticulum (27) (Fig. 3A). The behavior of the *Hs*NPC1–*Dr*C chimera in cells resembled that of WT *Hs*NPC1 and not *Hs*NPC1(I1061T), indicating that it too localizes to endo/lysosomal compartments (Fig. 3A). This localization was further confirmed by transiently expressing the NPC1 constructs in a U2OS NPC1-/- cell line in which we could detect co-localization with the endo/lysosomal marker, LAMP1 (Fig. 3B) (Spence et al., in press). These results suggest that *Dr*NPC1 domain C is correctly folded and does not interfere with the correct folding and trafficking of full-length *Hs*NPC1–*Dr*C.

We next monitored the cholesterol clearance activity of each protein upon stable expression in the NPC1-null Chinese hamster ovary (CHO) M12 cell line (Fig. 3C). Filipin, a fluorescent probe for free cholesterol, extensively stained the cholesterol-laden endo/lysosomal compartments of the parental M12 cells, as shown previously (26). Ectopic *Hs*NPC1 expression could clear this accumulated cholesterol, as previously described (20), substantially reducing filipin staining. Remarkably, *Hs*NPC1–*Dr*C could rescue cholesterol clearance as efficiently as WT *Hs*NPC1 (Fig. 3C). These findings affirm that *Dr*NPC1 domain C is biologically active and competent to perform a major housekeeping function of its human counterpart, despite its divergence from the latter at 48 out of 248 amino acid positions.

Finally, we challenged M12 cell lines expressing WT *Hs*NPC1 or *Hs*NPC1–*Dr*C with authentic EBOV (Fig. 3D). Replacement of human domain C with its Russell's viper ortholog reduced EBOV infection by almost three orders of magnitude. Similar results were obtained in infections with rVSV-EBOV GP (Fig. 3E), confirming that the *Dr*NPC1 domain C-imposed infection block occurs at the viral entry step. Taken together, these observations afford two conclusions. First, the failure of *Dr*NPC1 to support EBOV entry and infection arises at least in part because its domain C cannot bind to EBOV GP_{CL}. Second, one or more differences between the domain C sequences of *Hs*NPC1 and *Dr*NPC1 renders *Dr*NPC1 bereft of viral receptor activity without perturbing its normal function in cellular cholesterol homeostasis.

Differences in *N*–glycosylation do not explain the defect in EBOV GP_{CL}–*Dr*NPC1 domain C binding. To uncover the molecular basis of *Dr*NPC1's defective viral receptor function, we engineered and tested a panel of mutant, soluble NPC1 domain C constructs in both *Hs*NPC1 and *Dr*NPC1 backgrounds. We first considered the possibility that one or more differences in *N*–linked glycosylation sites determines the *Hs*NPC1–*Dr*NPC1 difference, because it is either re-

quired for GP_{CL}–*Hs*NPC1 binding or deleterious for GP_{CL}–*Dr*NPC1 binding (Fig. 4). Six sequons are conserved between the two proteins, but *Dr*NPC1 and *Hs*NPC1 domain C contain two and one unique sequons, respectively. Accordingly, we generated soluble domain C proteins containing or lacking each unique sequon and tested these putative gain-of-function and loss-of-function mutants for binding to EBOV GP_{CL}. 'Humanized' *Dr*NPC1 domain C proteins engineered to lack their unique sequons at positions 414 or 498 (*Hs*NPC1 numbering) or to gain the sequon at position 598 of *Hs*NPC1 remained defective at EBOV GP_{CL} binding in the ELISA. Conversely, *Hs*NPC1 domain C proteins engineered to resemble *Dr*NPC1 at each of these three positions remained fully competent to bind to EBOV GP_{CL}. Therefore, differences in *N*–linked glycosylation between the domain Cs of *Hs*NPC1 and *Dr*NPC1 do not account for the defective EBOV receptor activity of *Dr*NPC1.

A single point mutation renders *Dr*NPC1 domain C competent to bind to EBOV GP_{CL}. Having ruled out a role for variations in *N*–glycosylation, we next adopted a systematic approach to identify determinative sequences in NPC1 domain C. We expressed a series of soluble *Hs*NPC1–*Dr*NPC1 domain C chimeras, and measured their activity in the GP_{CL}-binding ELISA (Fig. 5). However only chimera 2, *Dr*NPC1 domain C containing *Hs*NPC1 residues 476–536, afforded GP_{CL}–NPC1 binding (Fig. 5A).

Chimera 2 introduced 14 Russell's viper→human amino acid changes into *Dr*NPC1. To further dissect their roles, we generated and tested three additional chimeras containing subsets of these amino acid changes (chimeras 4–6, Fig. 5B) in the GP_{CL} binding ELISA. The sub-region chimera 5 fully reconstituted GP_{CL}–*Dr*NPC1 domain C binding, providing evidence that one or more of the 6 *Hs*NPC1 residues in this construct confers gain of function to *Dr*NPC1.

To assess the individual contributions of the six Russell's viper→human amino acid changes in chimera 5, we separately introduced these changes into soluble *Dr*NPC1 domain C, and tested the capacity of each point mutant to bind to EBOV GP_{CL} by ELISA (Fig. 6). A single conservative mutation, Tyr 503→Phe, fully restored GP_{CL}–*Dr*NPC1 domain C binding, whereas the other 5 mutations had no discernible effect. Thus, the presence of Tyr instead of Phe at position 503 appears to completely explain the failure of *Dr*NPC1 to bind to EBOV GP_{CL}.

Phe ! Tyr sequence change at residue 503 controls NPC1's function as an EBOV entry receptor without affecting its housekeeping function. We postulated that the Phe↔Tyr sequence change at residue 503 might influence EBOV GP_{CL}–NPC1 binding in a bidirectional manner. Accordingly, we expressed and purified the reciprocal *Dr*NPC1(Y503F) and *Hs*NPC1(F503Y) domain C mutants, and tested them in the GP_{CL} binding ELISA (Fig. 7). Purified *Dr*NPC1(Y503F) domain C bound almost as well as its human counterpart to EBOV GP_{CL} (binding EC_{50}≈3 nM [Russell's viper] vs. 0.5 nM [human]). Conversely, no detectable GP_{CL} binding was obtained with the *Hs*NPC1(F503Y) domain C protein (EC_{50} > 1 μM).

To examine the consequences of the 503(Phe↔Tyr) sequence change for the cellular and viral receptor functions of NPC1, we introduced the F503Y and Y503F mutations into full-length *Hs*NPC1 and the seamless *Hs*NPC1-*Dr*C chimera, respectively, and expressed them stably in M12 NPC1-null cells (Fig. 8). Immunostaining of NPC1 in these cell lines revealed punctate, perinuclear staining resembling that observed for WT *Hs*NPC1 and *Hs*NPC1-*Dr*C (Figs. 8A and 3A), as well as colocalization with LAMP1 in transiently transfected U2OS NPC1-/- cell lines (Figs. 8B and 3B). Furthermore, filipin staining showed little or no cholesterol accumulation in cells expressing *Hs*NPC1(F503Y) or *Hs*NPC1-*Dr*C(Y503F) (Fig. 8B). Therefore, the F503Y and

Y503F mutations do not substantially affect the folding, endosomal delivery, and cholesterol clearance function of NPC1.

Finally, we challenged cell lines expressing the 503(Phe↔Tyr) NPC1 mutants with authentic EBOV and rVSV-EBOV-GP (Fig. 8C). The capacities of both authentic and surrogate viruses to enter and infect these cells were fully congruent with the results of the GP binding experiments. The viper→human Y503F mutation afforded the complete restoration of viral infection in cells expressing the *Hs*NPC1-*Dr*C chimera (≈100,000% increase). Reciprocally, the human→viper F503Y mutation reduced viral infection in cells expressing *Hs*NPC1 by ≈99%. Thus, the infection data correlate with the GP_{CL}-domain C binding data, demonstrating that switching the residue at position 503 changes the ability of human and Russell's viper NPC1 domain C to bind EBOV GP_{CL}, thereby determining the ability of these NPC1 proteins to be used as EBOV receptors.

A bulky, hydrophobic amino acid residue at position 503 favors EBOV GP_{CL}-NPC1 domain C binding. To determine the mechanism by which the change in NPC1 residue 503 controls binding of *Hs*NPC1 to EBOV GP_{CL}, we engineered a series of NPC1 domain C proteins bearing amino acid residues with divergent physicochemical properties at position 503. Examination of these mutants by GP_{CL} binding ELISA revealed that binding avidity generally correlated with amino acid size and polarity (Fig. 9A). Specifically, residues with bulky, hydrophobic side chains (Leu, Trp) afforded GP_{CL}-NPC1 binding at WT levels, whereas residues with polar side chains (Asp, His, Ser) completely abrogated binding. Binding was greatly reduced, but detectable, with Ala and Thr at residue 503. The recently solved structure of EBOV GP_{CL} bound to NPC1 domain C shows that this residue inserts into the hydrophobic trough of EBOV GP_{CL} (28, 29) similar to residue F225 of the EBOV glycan cap (Fig. 9B, 9C, (25)).

The tyrosine residue at position 503 controls EBOV GP_{CL} binding function in reptile NPC1 domain C orthologs. Finally, we asked if our findings had implications for host cell range in other vertebrates, especially reptiles, which appear to be refractory to infection by EBOV (8, 30). An alignment of available NPC1 domain C sequences from a panel of vertebrate species revealed that, although there exists a number of differences in amino acid sequence around residue 503, the Phe at this position is itself very well conserved among vertebrates, with only two *NPC1* orthologs—those of the Russell's viper and king cobra (*Ophiaphagus hannah*)— encoding a Tyr at this position (Fig. 10A). Interestingly, the predicted NPC1 polypeptide sequences of two additional snakes, the Burmese python (*Python bivittatus*) and the common garter snake (*Thamnophis sirtalis*), encode a Phe at position 503 (Fig. 10A). To investigate the GP_{CL}-binding capacities of the snake NPC1 orthologs, we expressed and purified soluble NPC1 domain C proteins for the king cobra and Burmese python, and tested them for binding to EBOV GP_{CL}. The capacity of these proteins to bind to EBOV GP_{CL} was concordant with the identity of the residue at NPC1 codon 503. Thus, king cobra NPC1 domain C (Tyr 503) resembled viper NPC1 domain C in its inability to bind to EBOV GP_{CL}, whereas Burmese python NPC1 domain C (503 Phe) readily bound to EBOV GP_{CL} (Fig. 10B). We tested two more reptilian NPC1 orthologs—from Chinese softshell turtle and Carolina anole (both encoding Phe at position 503), and found that they could all bind to EBOV GP_{CL} (Fig. 10C). These findings provide additional evidence that *NPC1* residue 503 influences the cellular host range of EBOV at the level of virus-receptor recognition, and raise the possibility that sequence differences at this position influence the susceptibility of reptiles to filovirus infection in nature.

Discussion

The essential entry receptor NPC1 is the first known molecular determinant of the cellular host range of EBOV and other filoviruses (24). In this study, we uncover one mechanism by which NPC1 imposes a species-specific barrier to EBOV infection. We show that reptilian cells derived from the Russell's viper, *Daboia russellii*, are largely resistant to EBOV entry and infection because of the presence of a Tyr residue at position 503 in NPC1, whereas the NPC1 orthologs of most other types of animals, include humans, carry a highly conserved Phe residue. Unexpectedly, toggling this residue between Phe and Tyr in either human or viper NPC1 backgrounds switched each protein's ability to act as an EBOV receptor. NPC1's crucial housekeeping function–distribution of cholesterol from the endo/lysosomal compartment to other cellular membranes–remained unaffected by these changes. Thus, our work identifies a genetic determinant in NPC1 that controls its viral receptor function, and consequently, host susceptibility to EBOV infection, in a manner that is selective, yet transferable between highly divergent NPC1 orthologs.

The determinative Phe 503→Tyr change is located in NPC1's second luminal domain (C), which directly binds to a cleaved form of the EBOV entry glycoprotein (GP_{CL}) during viral entry (22, 23, 25). Here, we found that Phe 503→Tyr renders cells non-permissive to EBOV infection because it reduces the apparent binding affinity of GP_{CL} for NPC1 domain C by more than 1000-fold. What mechanism might account for this extraordinary effect of a single hydroxyl group on virus-receptor interaction?

The recently solved structure of the EBOV GP_{CL} bound to NPC1 domain C reveals that Phe 503 in human NPC1 domain C inserts deeply into the hydrophobic GP_{CL} trough during GP-NPC1 interaction, in a manner that resembles the interaction of Phe 225 in the GP glycan cap with the GP_{CL} trough in uncleaved GP (Fig. 9B) (25). The introduction, at position 503, of a po-

277 lar hydroxyl group (Tyr) or other polar side chains (Asp, His, Ser, Gly) is likely to be energeti-
278 cally unfavorable, thereby reducing the affinity of GP_{CL} -NPC1 binding.

279 We recently demonstrated that the residue 502 in NPC1 was under positive selection in
280 bats, and was responsible for the reduced susceptibility of African straw-colored fruit bat cells to
281 EBOV infection (24). Since none of the bat species encodes a Tyr at position 503 in NPC1, there
282 was no observed signature of positive selection at this residue. The structure rationalizes the ef-
283 fect of these residues on GP-NPC1 binding, as both are located in the α4– α5 loop of NPC1 do-
284 main C that directly interacts with EBOV GP_{CL} ('loop 2'; (25)).

285 It is unclear what relationships, if any, exist (or have existed) in nature between filoviruses
286 and snakes or other reptiles. Experimental infections of wild-caught reptiles and amphibians by
287 Swanepoel and colleagues (30) showed a general refractoriness to EBOV infection or replica-
288 tion, but minimal titers were recovered on a few occasions from the brown house snake (*Lam-*
289 *prophis fuliginosus*). Following outbreaks of the Ebola relative, Marburg virus (MARV) at the
290 mine in Kitaka Cave, the nearby "Python cave" in Queen Elizabeth National Park in Uganda (31,
291 32) and the Goroumbwa Mine in the Democratic Republic of Congo (33), a number of Egyptian
292 fruit bats found to be infected with MARV (5, 6, 34). Unfortunately, though the African Rock
293 python (*Python sebae*) and forest cobras (*Naja melanoleuca*) are part of the fauna in these loca-
294 tions, there were no reports on investigations on snakes from these caves for filovirus infec-
295 tion(33), (6). Nevertheless, our finding that two snake NPC1 orthologs are nonpermissive to filo-
296 virus entry and infection due to a single amino acid change leads us to speculate that this change
297 was an adaptation to reduce infection by a filovirus, thereby increasing host survivability. More
298 extensive wildlife sampling coupled with genetic and functional analysis of host-virus interac-
299 tions associated with filovirus infection may uncover additional evidence for evolutionary arms

300 races between filoviruses and multiple types of animals (bats, reptiles, rodents).

301 **Materials and Methods:**

302 **Cells**

303 Vero grivet and HEK 293T cells were maintained in high-glucose Dulbecco's modified Eagle
304 medium (DMEM; Thermo Fisher Scientific, Waltham MA) supplemented with 10% fetal bovine
305 serum (FBS; Atlanta Biologicals, Flowery Branch, GA) and 1% penicillin-streptomycin (Thermo
306 Fisher Scientific) at 37˚C and 5% CO_2. Chinese hamster ovary (CHO) cells were maintained in
307 DMEM-Ham's F-12 medium (50/50 mix) (Thermo Fisher Scientific) supplemented with 10%
308 FBS at 37˚C and 5% CO_2. Cell lines were generated by retroviral transduction system, as previ-
309 ously described (22), to stably overexpress the NPC1 constructs in CHO-M12 cells, which con-
310 tain a deletion in the NPC1 locus (26) (transient transfections of NPC1 constructs + LAMP1 for
311 colocalization experiments). FreeStyle™ 293-F cells were maintained in GIBCO FreeStyle™
312 293 expression medium (Thermo Fisher Scientific) at 37˚C and 8% CO_2.
313
314 **NPC1 constructs**
315 NPC1 domain C sequences (residues 373 to 620) flanked by sequences that form anti-parallel
316 coiled coils as previously described (35), were cloned into the pcDNA3.1(+) vector. Constructs
317 made were included glycosylation mutants in *Hs*NPC1 domain C: L414N+D416T,
318 K498N+G500S and N598A, while those in *Dr*NPC1 domain C: N414A, N498A and R600T.
319 *Dr*NPC1 domain C chimeras were made by substituting these residues for human residues: 373-
320 475 (chimera 1), 476-536 (chimera 2), 537-620 (chimera 3), 493-502 (chimera 4), 502-512 (chi-
321 mera 5) and 513-522 (chimera 6), and point mutations made were E502D, Y503F, I505V,
322 H506Y, F509Y and S511T. The constructs were then transiently transfected into HEK 293T

cells and the supernatant with secreted protein was harvested after 72h and used in ELISA assays. Purified proteins were made by transfecting FreeStyle™ 293-F cells in suspension, harvested 72 h post-transfection and purifying by incubation with His-60 Nickel resin. The proteins were eluted at 500mM imidazole and pH 7.6, and dialyzed into 50mM MES, 150mM NaCl, pH5.5. Domain C chimeras in the full length NPC1 were generated by seamlessly replacing the domain C sequences in the *Hs*NPC1. The constructs were subcloned into the pBABE-puro retroviral vector and stably transfected into CHO-M12 cells by retroviral transduction, as previously described (22). All constructs possessed *N*–terminal flag tags.

VSV pseudotype infections

Replication-incompetent vesicular stomatitis Indiana virus (VSV) pseudotypes encoding eGFP in the first position and EBOV GP in place of VSV G were made as previously described (9, 36). EBOV GPΔMuc matches the EBOV/H.sapiens-tc/COD/1976/Yambuku-Mayinga isolate amino acid sequence (GenBank accession number AF086833), but lacks the mucin-like domain (Δ309–489; ΔMuc) (37). Unless otherwise indicated, viruses were titered on Vero grivet monkey cells by manual counting of eGFP-positive cells. Cleaved EBOV GP (GP_{CL}) was generated *in vitro* using the bacterial protease thermolysin (250μg/mL) (Sigma-Aldrich, St Louis, MO) for 1h at 37˚C as described previously (38, 39), and the reaction was stopped by adding the metalloprotease inhibitor phosphoramidon (1mM) (Sigma-Aldrich).

Authentic Ebola virus infections

CHO cells, seeded in black Cellcoat® 96 well plates (Greiner Bio-One North America, Monroe, NC) were incubated with Ebola virus/H.sapiens-tc/COD/1995/Kikwit-9510621 at the indicated

multiplicity of infection in a biosafety level 4 (BSL-4) laboratory located at USAMRIID. Following 1h absorption, virus inoculum was removed and cells were washed once with PBS. Cells were then incubated at 37˚C, 5% CO_2, 80% humidity for 72h, at which time, the cells were washed once with PBS and submerged in 10% formalin prior to removal from the BSL-4 laboratory. Formalin was removed and cells were washed 3 times with PBS. Cells were blocked by adding 3% BSA/PBS to each well and incubating at 37˚C for 2h. Cells were incubated with EBOV GP-specific mAb KZ52, diluted to 1µg/mL in 3% BSA/PBS, at room temperature for 2h. Cells were washed 3 times with PBS prior to addition of goat anti-human IgG-AlexaFluor 488 (Thermo Fisher Scientific) secondary antibody. Following 1h incubation with secondary antibody, cells were washed 3 times prior to addition of Hoechst 33342 (Thermo Fisher Scientific) diluted in PBS. Cells were imaged and percent of virus infected cells calculated using the Operetta High Content Imaging System (PerkinElmer, Waltham, MA) and Harmony® High Content Imaging and Analysis Software (PerkinElmer).

GP_{CL} –NPC1 domain C capture ELISA

Normalization of NPC1 domain C supernatants and proteins was carried out as previously described (24): resolving on SDS-PAGE followed by immunoblotting with anti-flag primary antibody (Sigma Aldrich) and anti-mouse Alexa-680 secondary antibody (Thermo Fisher Scientific), and quantified on the LI-COR Odyssey Imager (LI-COR Biosciences, Lincoln, NE). Capture ELISAs were also performed as previously described (22, 24). Briefly, high-binding 96-well ELISA plates (Corning, Corning, NY) were coated with KZ52 (40) (2µg/mL in PBS) and then blocked using PBS containing 3% bovine serum albumin (PBSA). Pseudotyped EBOV was cleaved with thermolysin (250µg/mL) at 37˚C for 1h and captured on the plate. Unbound virus

was washed off and serial dilutions of either flag-tagged purified soluble NPC1 domain C (domain C; 0–40μg/mL), or supernatants from transient transfections of the NPC1 constructs on HEK 293T cells were added. Bound domain C was detected by a horseradish conjugated anti-flag antibody, and Ultra-TMB substrate (ThermoFisher). EC_{50} values were calculated from binding curves generated by non-linear regression analysis using Prism (GraphPad Software, La Jolla CA). Binding ELISAs were done in duplicate, and in at least two independent experiments. All incubation steps were done at 37˚C for 1 hour or at 4˚C overnight.

Immunofluorescence

Imaging was performed in U2OS or CHO cells grown on 12-mm coverslips and fixed with 4% paraformaldehyde. For antibody staining, the coverslips were incubated with an anti-flag antibody (Sigma Aldrich) in PBS containing 0.1% Triton X-100 and 1% BSA. Detection was by incubation with Alexa 488-conjugated secondary antibodies (Thermo Fisher Scientific). For filipin staining, the coverslips were stained with 50μg/mL of *Streptomyces filipensis* filipin III complex (Sigma Aldrich) in PBS for 1h. Coverslips were mounted on glass slides using ProLong antifade reagent (Thermo Fisher Scientific) and images were acquired with an inverted fluorescence microscope equipped with a 63X high-numerical aperture oil objective.

Acknowledgments

We thank Tyler Krause, Cecelia Harold, and Tanwee Alkutkar for excellent technical support. We are grateful to Jens H. Kuhn for comments on a preliminary version of this manuscript. We are grateful to T. Y. Chang for his gift of CHO M12 cells.

Supported by grants from the U.S. National Institutes of Health (AI101436 to K.C.), and

the U.S. Defense Threat Reduction Agency (CB3948 to J.M.D.). K.C. is additionally supported by a Harold and Muriel Block Faculty Scholarship and an Irma T. Hirschl/Monique Weill-Caulier Research Award at the Albert Einstein College of Medicine. Opinions, conclusions, interpretations, and recommendations are those of the authors and are not necessarily endorsed by the U.S. Department of the Army and the U.S. Department of Defense.

References:

1. **Baize S**, **Pannetier D**, **Oestereich L**, **Rieger T**, **Koivogui L**, **Magassouba N**, **Soropogui B**, **Sow MS**, **Keita S**, **De Clerck H**, **Tiffany A**, **Dominguez G**, **Loua M**, **Traoré A**, **Kolié M**, **Malano ER**, **Heleze E**, **Bocquin A**, **Mély S**, **Raoul H**, **Caro V**, **Cadar D**, **Gabriel M**, **Pahlmann M**, **Tappe D**, **Schmidt-Chanasit J**, **Impouma B**, **Diallo AK**, **Formenty P**, **Van Herp M**, **Günther S**. 2014. Emergence of Zaire Ebola virus disease in Guinea. N Engl J Med **371**:1418–1425.

2. **La Vega de M-A**, **Stein D**, **Kobinger GP**. 2015. Ebolavirus Evolution: Past and Present. PLoS Pathog **11**:e1005221.

3. **Negredo A**, **Palacios G**, **Vázquez-Morón S**, **González F**, **Dopazo H**, **Molero F**, **Juste J**, **Quetglas J**, **Savji N**, **la Cruz Martínez de M**, **Herrera JE**, **Pizarro M**, **Hutchison SK**, **Echevarría JE**, **Lipkin WI**, **Tenorio A**. 2011. Discovery of an Ebolavirus-Like Filovirus in Europe. PLoS Pathog **7**:e1002304.

4. **Leroy EM**, **Kumulungui B**, **Pourrut X**, **Rouquet P**, **Hassanin A**, **Yaba P**, **Délicat A**, **Paweska JT**, **Gonzalez J-P**, **Swanepoel R**. 2005. Fruit bats as reservoirs of Ebola virus. Nature **438**:575–576.

5. **Towner JS**, **Pourrut X**, **Albariño CG**, **Nkogue CN**, **Bird BH**, **Grard G**, **Ksiazek TG**, **Gonzalez J-P**, **Nichol ST**, **Leroy EM**. 2007. Marburg virus infection detected in a common African bat. PLoS ONE **2**:e764.

6. **Towner JS**, **Amman BR**, **Sealy TK**, **Carroll SAR**, **Comer JA**, **Kemp A**, **Swanepoel R**, **Paddock CD**, **Balinandi S**, **Khristova ML**, **Formenty PBH**, **Albariño CG**, **Miller DM**, **Reed ZD**, **Kayiwa JT**, **Mills JN**, **Cannon DL**, **Greer PW**, **Byaruhanga E**, **Farnon EC**, **Atimnedi P**, **Okware S**, **Katongole-Mbidde E**, **Downing R**, **Tappero JW**, **Zaki SR**, **Ksiazek TG**, **Nichol ST**, **Rollin PE**. 2009. Isolation of genetically diverse Marburg viruses from Egyptian fruit bats. PLoS Pathog **5**:e1000536.

7. **Feldmann H**, **Geisbert TW**. 2011. Ebola haemorrhagic fever. The Lancet **377**:849–862.

8. **Van der Groen G**, **Webb P**, **Johnson K**, **Lange JV**, **Lindsay H**, **Eliott L**. 1978. Growth

of Lassa and Ebola viruses in different cell lines, pp. 172–176. *In* Pattyn, SR (ed.), Ebola virus haemorrhagic fever. Elsevier/North-Holland Biomedical Press.

9. **Takada A**, **Robison C**, **Goto H**, **Sanchez A**, **Murti KG**, **Whitt MA**, **Kawaoka Y**. 1997. A system for functional analysis of Ebola virus glycoprotein. Proc Natl Acad Sci USA **94**:14764–14769.

10. **Wool-Lewis RJ**, **Bates P**. 1998. Characterization of Ebola Virus Entry by Using Pseudotyped Viruses: Identification of Receptor-Deficient Cell Lines. Journal of Virology **72**:3155–3160.

11. **Li F**. 2013. Receptor recognition and cross-species infections of SARS coronavirus. Antiviral Research **100**:246–254.

12. **Sheahan T**, **Rockx B**, **Donaldson E**, **Corti D**, **Baric R**. 2008. Pathways of cross-species transmission of synthetically reconstructed zoonotic severe acute respiratory syndrome coronavirus. Journal of Virology **82**:8721–8732.

13. **Hueffer K**, **Parker JSL**, **Weichert WS**, **Geisel RE**, **Sgro J-Y**, **Parrish CR**. 2003. The natural host range shift and subsequent evolution of canine parvovirus resulted from virus-specific binding to the canine transferrin receptor. Journal of Virology **77**:1718–1726.

14. **Radoshitzky SR**, **Kuhn JH**, **Spiropoulou CF**, **Albariño CG**, **Nguyen DP**, **Salazar-Bravo J**, **Dorfman T**, **Lee AS**, **Wang E**, **Ross SR**, **Choe H**, **Farzan M**. 2008. Receptor determinants of zoonotic transmission of New World hemorrhagic fever arenaviruses. Proceedings of the National Academy of Sciences **105**:2664–2669.

15. **Abraham J**, **Corbett KD**, **Farzan M**, **Choe H**, **Harrison SC**. 2010. Structural basis for receptor recognition by New World hemorrhagic fever arenaviruses. Nat Struct Mol Biol **17**:438–444.

16. **Wang E**, **Albritton L**, **Ross SR**. 2006. Identification of the segments of the mouse transferrin receptor 1 required for mouse mammary tumor virus infection. J Biol Chem **281**:10243–10249.

17. **Allison AB**, **Harbison CE**, **Pagan I**, **Stucker KM**, **Kaelber JT**, **Brown JD**, **Ruder MG**, **Keel MK**, **Dubovi EJ**, **Holmes EC**, **Parrish CR**. 2012. Role of multiple hosts in the cross-species transmission and emergence of a pandemic parvovirus. Journal of Virology **86**:865–872.

18. **Demogines A**, **Abraham J**, **Choe H**, **Farzan M**, **Sawyer SL**. 2013. Dual host-virus arms races shape an essential housekeeping protein. PLoS Biol **11**:e1001571.

19. **Jae LT**, **Raaben M**, **Herbert AS**, **Kuehne AI**, **Wirchnianski AS**, **Soh TK**, **Stubbs SH**, **Janssen H**, **Damme M**, **Saftig P**, **Whelan SP**, **Dye JM**, **Brummelkamp TR**. 2014. Virus entry. Lassa virus entry requires a trigger-induced receptor switch. Science **344**:1506–1510.

20. **Carette JE**, **Raaben M**, **Wong AC**, **Herbert AS**, **Obernosterer G**, **Mulherkar N**, **Kuehne AI**, **Kranzusch PJ**, **Griffin AM**, **Ruthel G**, **Cin PD**, **Dye JM**, **Whelan SP**, **Chandran K**, **Brummelkamp TR**. 2011. Ebola virus entry requires the cholesterol transporter Niemann-Pick C1. Nature **477**:340–343.

21. **Côté M**, **Misasi J**, **Ren T**, **Bruchez A**, **Lee K**, **Filone CM**, **Hensley L**, **Li Q**, **Ory D**, **Chandran K**, **Cunningham J**. 2011. Small molecule inhibitors reveal Niemann-Pick C1 is essential for Ebola virus infection. Nature **477**:344–348.

22. **Miller EH**, **Obernosterer G**, **Raaben M**, **Herbert AS**, **Deffieu MS**, **Krishnan A**, **Ndungo E**, **Sandesara RG**, **Carette JE**, **Kuehne AI**, **Ruthel G**, **Pfeffer SR**, **Dye JM**, **Whelan SP**, **Brummelkamp TR**, **Chandran K**. 2012. Ebola virus entry requires the host-programmed recognition of an intracellular receptor. EMBO J 1–14.

23. **Krishnan A**, **Miller E**, **Herbert A**, **Ng M**, **Ndungo E**, **Whelan S**, **Dye J**, **Chandran K**. 2012. Niemann-Pick C1 (NPC1)/NPC1-like1 Chimeras Define Sequences Critical for NPC1's Function as a Filovirus Entry Receptor. Viruses **4**:2471–2484.

24. **Ng M**, **Ndungo E**, **Kaczmarek ME**, **Herbert AS**, **Binger T**, **Kuehne AI**, **Jangra RK**, **Hawkins JA**, **Gifford RJ**, **Biswas R**, **Demogines A**, **James RM**, **Yu M**, **Brummelkamp TR**, **Drosten C**, **Wang L-F**, **Kuhn JH**, **Müller MA**, **Dye JM**, **Sawyer SL**, **Chandran K**. 2015. Filovirus receptor NPC1 contributes to species-specific patterns of ebolavirus susceptibility in bats. Elife **4:e11785**.

25. **Wang H**, **Shi Y**, **Song J**, **Qi J**, **Lu G**, **Yan J**, **Gao GF**. 2016. Ebola Viral Glycoprotein Bound to Its Endosomal Receptor Niemann-Pick C1. Cell **164**:258–268.

26. **Millard EE**, **Srivastava K**, **Traub LM**, **Schaffer JE**, **Ory DS**. 2000. Niemann-pick type C1 (NPC1) overexpression alters cellular cholesterol homeostasis. J Biol Chem **275**:38445–38451.

27. **Gelsthorpe ME**, **Baumann N**, **Millard E**, **Gale SE**, **Langmade SJ**, **Schaffer JE**, **Ory DS**. 2008. Niemann-Pick type C1 I1061T mutant encodes a functional protein that is selected for endoplasmic reticulum-associated degradation due to protein misfolding. J Biol Chem **283**:8229–8236.

28. **Lee JE**, **Fusco ML**, **Hessell AJ**, **Oswald WB**, **Burton DR**, **Saphire EO**. 2008. Structure of the Ebola virus glycoprotein bound to an antibody from a human survivor. Nature **454**:177–182.

29. **Bornholdt ZA**, **Ndungo E**, **Fusco ML**, **Flyak AI**, **Crowe JE**, **Chandran K**, **Saphire EO**. Host-primed Ebola virus GP exposes a hydrophobic NPC1 receptor-binding pocket, revealing a target for broadly neutralizing antibodies. MBio. In press

30. **Swanepoel R**, **Leman PA**, **Burt FJ**, **Zachariades NA**, **Braack LEO**, **Ksiazek TG**, **Rollin PE**, **Zaki SR**, **Peters CJ**. 1996. Experimental inoculation of plants and animals with Ebola virus. Emerg Infect Dis **2**:321–325.

31. **Adjemian J**, **Farnon EC**, **Tschioko F**, **Wamala JF**, **Byaruhanga E**, **Bwire GS**, **Kansiime E**, **Kagirita A**, **Ahimbisibwe S**, **Katunguka F**, **Jeffs B**, **Lutwama JJ**, **Downing R**, **Tappero JW**, **Formenty P**, **Amman B**, **Manning C**, **Towner J**, **Nichol ST**, **Rollin PE**. 2011. Outbreak of Marburg hemorrhagic fever among miners in Kamwenge and Ibanda Districts, Uganda, 2007. Journal of Infectious Diseases **204 Suppl 3**:S796–9.

32. **Timen A**, **Koopmans MPG**, **Vossen ACTM**, **van Doornum GJJ**, **Günther S**, **van den Berkmortel F**, **Verduin KM**, **Dittrich S**, **Emmerich P**, **Osterhaus ADME**, **van Dissel JT**, **Coutinho RA**. 2009. Response to imported case of Marburg hemorrhagic fever, the Netherland. Emerg Infect Dis **15**:1171–1175.

33. **Swanepoel R**, **Smit SB**, **Rollin PE**, **Formenty P**, **Leman PA**, **Kemp A**, **Burt FJ**, **Grobbelaar AA**, **Croft J**, **Bausch DG**, **Zeller H**, **Leirs H**, **Braack L**, **Libande ML**, **Zaki S**, **Nichol ST**, **Ksiazek TG**, **Paweska JT**. 2007. Studies of Reservoir Hosts for Marburg Virus. Emerg Infect Dis **13**:1847–1851.

34. **Amman BR**, **Carroll SA**, **Reed ZD**, **Sealy TK**, **Balinandi S**, **Swanepoel R**, **Kemp A**, **Erickson BR**, **Comer JA**, **Campbell S**, **Cannon DL**, **Khristova ML**, **Atimnedi P**, **Paddock CD**, **Crockett RJK**, **Flietstra TD**, **Warfield KL**, **Unfer R**, **Katongole-Mbidde E**, **Downing R**, **Tappero JW**, **Zaki SR**, **Rollin PE**, **Ksiazek TG**, **Nichol ST**, **Towner JS**. 2012. Seasonal pulses of Marburg virus circulation in juvenile *Rousettus aegyptiacus* bats coincide with periods of increased risk of human infection. PLoS Pathog **8**:e1002877.

35. **Deffieu MS**, **Pfeffer SR**. 2011. Niemann-Pick type C 1 function requires lumenal domain residues that mediate cholesterol-dependent NPC2 binding. Proceedings of the National Academy of Sciences **108**:18932–18936.

36. **Chandran K**, **Sullivan NJ**, **Felbor U**, **Whelan SP**, **Cunningham JM**. 2005. Endosomal Proteolysis of the Ebola Virus Glycoprotein Is Necessary for Infection. Science **308**:1643–1645.

37. **Jeffers SA**, **Sanders DA**, **Sanchez A**. 2002. Covalent modifications of the ebola virus glycoprotein. Journal of Virology **76**:12463–12472.

38. **Schornberg K**, **Matsuyama S**, **Kabsch K**, **Delos S**, **Bouton A**, **White J**. 2006. Role of endosomal cathepsins in entry mediated by the Ebola virus glycoprotein. Journal of Virology **80**:4174–4178.

39. **Wong AC**, **Sandesara RG**, **Mulherkar N**, **Whelan SP**, **Chandran K**. 2010. A forward genetic strategy reveals destabilizing mutations in the Ebolavirus glycoprotein that alter its protease dependence during cell entry. Journal of Virology **84**:163–175.

40. **Maruyama T**, **Rodriguez LL**, **Jahrling PB**, **Sanchez A**, **Khan AS**, **Nichol ST**, **Peters CJ**, **Parren PWHI**, **Burton DR**. 1999. Ebola Virus Can Be Effectively Neutralized by Antibody Produced in Natural Human Infection. Journal of Virology **73**:6024–6030.

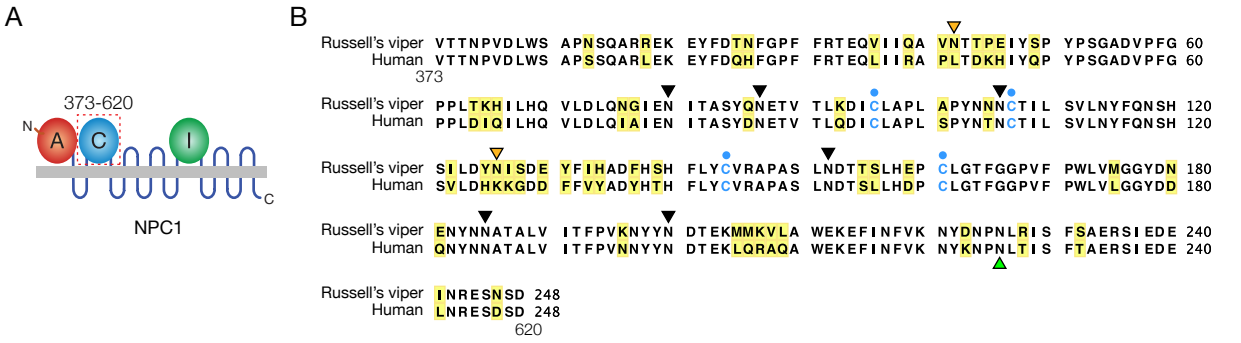

Fig 1: Alignment of human and viper NPC1 domain C. Alignment of NPC1 domain C sequences from human and Russell's viper. Non-identical residues are highlighted yellow. Cysteine residues are in blue. Predicted *N*-glycosylation sites that are conserved in both proteins are indicated with black arrows. Orange arrows mark those unique to Russell's viper NPC1 domain C, and a green arrow marks one that is unique to human NPC1 domain C.

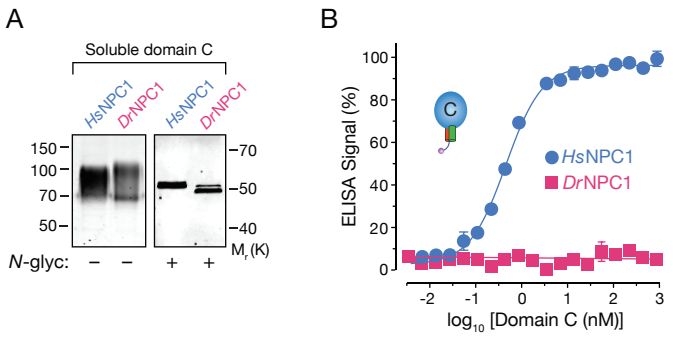

Fig 2: Both *Hs*NPC1 and *Dr*NPC1 domain C proteins are expressed and secreted but bind differentially to EBOV GP$_{CL}$. (A) Soluble forms of the NPC1 domain C proteins from human (***Hs***NPC1) and Russell's viper (*Dr*NPC1) were expressed in FreeStyle™ 293-F cells and purified by nickel-affinity chromatography. Equal concentrations were resolved by anti-flag immunostaining. Left, no treatment. Right, treated with protein *N*–glycosidase F. (B) The two NPC1 domain C proteins were tested in an ELISA for binding to EBOV GP$_{CL}$. VSV-EBOV GP viruses were cleaved with thermolysin (250µg/mL) and captured on an ELISA plate using the monoclonal antibody KZ52. Serial dilutions of either *Hs*NPC1 or *Dr*NPC1 domain C proteins were added, and binding to GP$_{CL}$ was detected by anti-flag antibody.

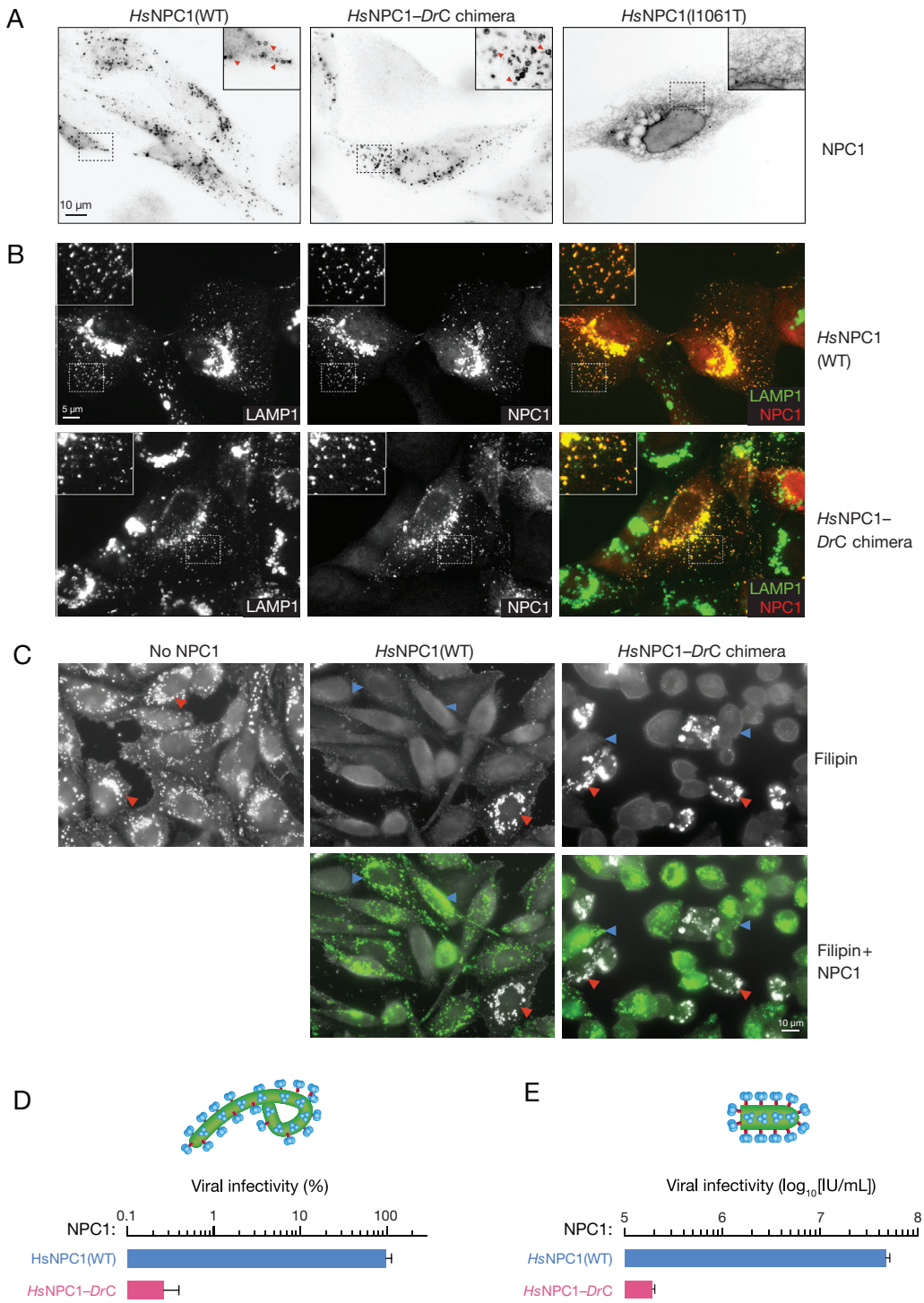

Fig 3: *Hs*NPC1-*Dr*C chimera is functional at cholesterol clearance from lysosomes, but does not support EBOV entry and infection. (A) Distribution of full length NPC1 constructs stably expressed in a CHO cell line that lacks a functional NPC1 (CHO-M12). *Hs*NPC1 and the human-viper chimera (*Hs*NPC1-*Dr*C) display a typical late endosomal/lysosomal localization pattern. In contrast, the mutant *Hs*NPC1(I1061T) is retained in the endoplasmic reticulum. (B) NPC1 constructs from (A) immunostained with anti-flag antibody (red), colocalize with the lysosomal marker, LAMP1 (green) when transiently expressed in U2OS cells. (C) CHO-M12 cells stably expressing either *Hs*NPC1 WT or *Hs*NPC1-*Dr*C were stained with filipin to visualize unesterified cholesterol. Top panel, filipin staining. Cholesterol-laden cells are marked with red arrows. Blue arrows indicate cells that are functional at cholesterol clearance. Bottom panel, cells immunostained with anti-flag antibody for NPC1 expression (green). (D) Infection of cells from (C) by authentic EBOV (MOI of 10), scored 72h post infection and normalized to infection on HsNPC1(WT). (D) Infection of cells from (C) by VSV-EBOV GP calculated by manual counting of eGFP positive cells. IU/mL, infectious units per mL.

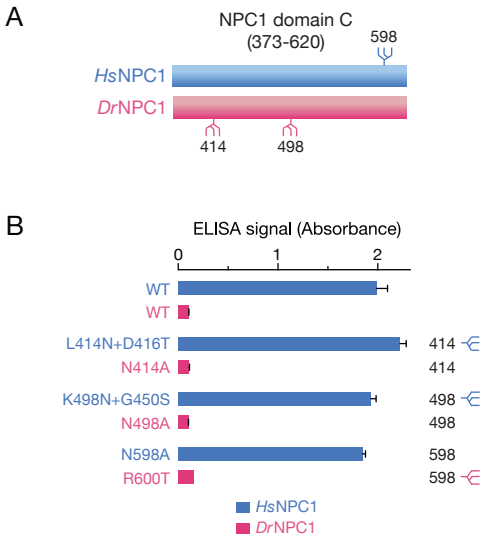

Fig 4: *N*–glycosylation of NPC1 domain C does not affect EBOV GP$_{CL}$ binding.
(A) Location of the three unique sequons in *Hs*NPC1 vs. *Dr*NPC1 domain C.
(B) Glycosylation mutants were made in both *Hs*NPC1 (losing sequon at position 598 and gaining sequons at position 414 and 498) and *Dr*NPC1 (losing sequons at osition 414 and 498 and gaining sequon at position 598). Domain C proteins were expressed in HEK 293T cells and tested for EBOV GP$_{CL}$ binding by ELISA

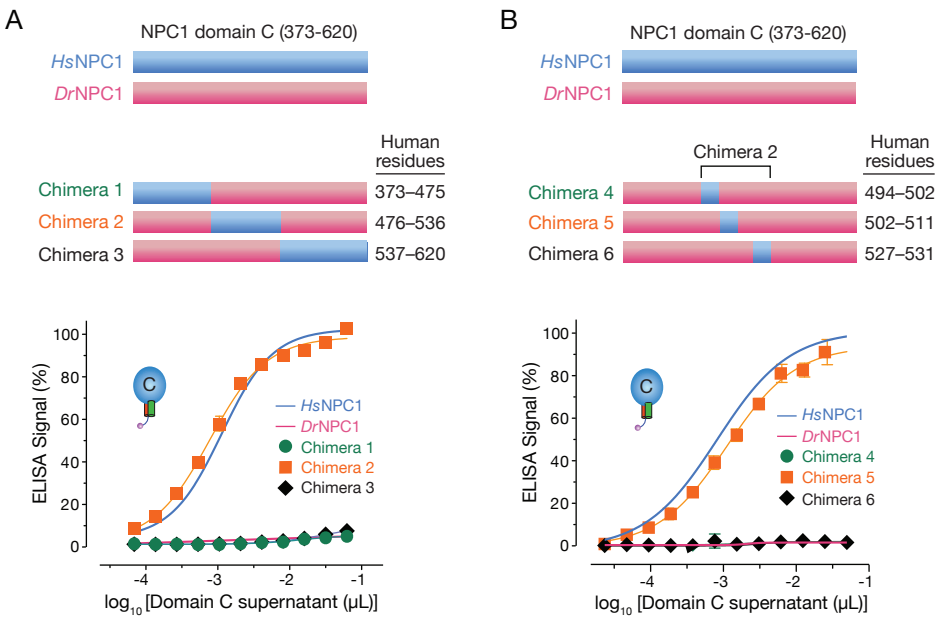

Fig 5: Middle region of *Hs*NPC1 domain C confers binding ability to *Dr*NPC1. (A) Chimeras were engineered by replacing *Dr*NPC1 domain C sequences with human sequences 373–475 (chimera 1), 476–536 (chimera 2) or 537–620 (chimera 3). The chimeras were expressed in HEK 293T cells and tested for EBOV GP_{CL} binding by ELISA. (B) Further dissection of chimera 2 was done by replacing smaller subsets of *Dr*NPC1 with human residues: 494–502 (chimera 4), 502–511 (chimera 5) and 527–531 (chimera 6). Chimeric NPC1 domain C proteins were tested as in (A).

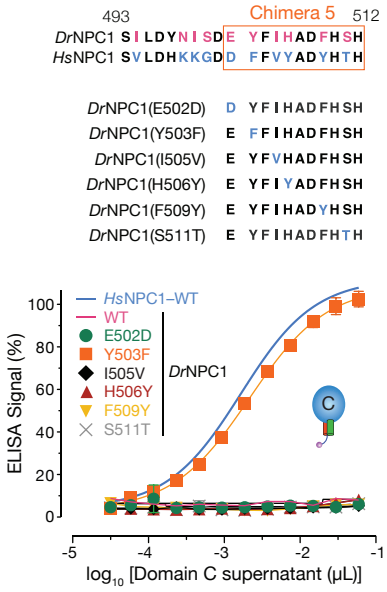

Fig 6: A single amino acid change renders *Dr*NPC1 domain C fully competent to bind EBOV GP$_{CL}$. Chimera 5 contains 6 amino acid differences between *Dr*NPC1 and *Hs*NPC1 domain C. Point mutations were made in the *Dr*NPC1 domain C by switching the viper amino acid residue at each of these positions to the corresponding human residue: E502D, Y503F, I505V, H506Y, F509Y and S511T. The point mutants were expressed in HEK 293T cells and tested for EBOV GP$_{CL}$ binding by ELISA.

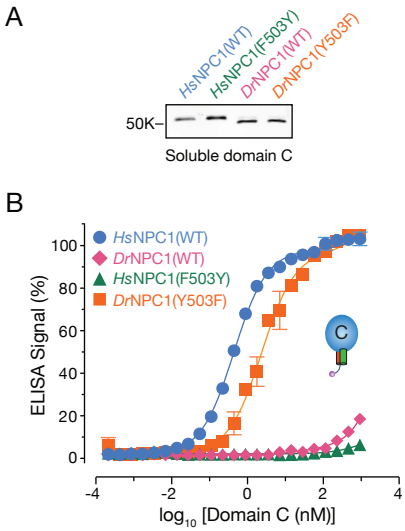

Fig 7: NPC1 residue 503 bidirectionally alters domain C's capacity to bind EBOV GP$_{CL}$. (A) *Hs*NPC1 and *Dr*NPC1 domain C proteins bearing point mutations at residue 503 (*Hs*NPC1, F503Y; *Dr*NPC1, Y503F) were expressed and purified. (B) Serial dilutions of equivalent amounts of purified NPC1 domain C proteins were tested for EBOV GPCL binding by ELISA.

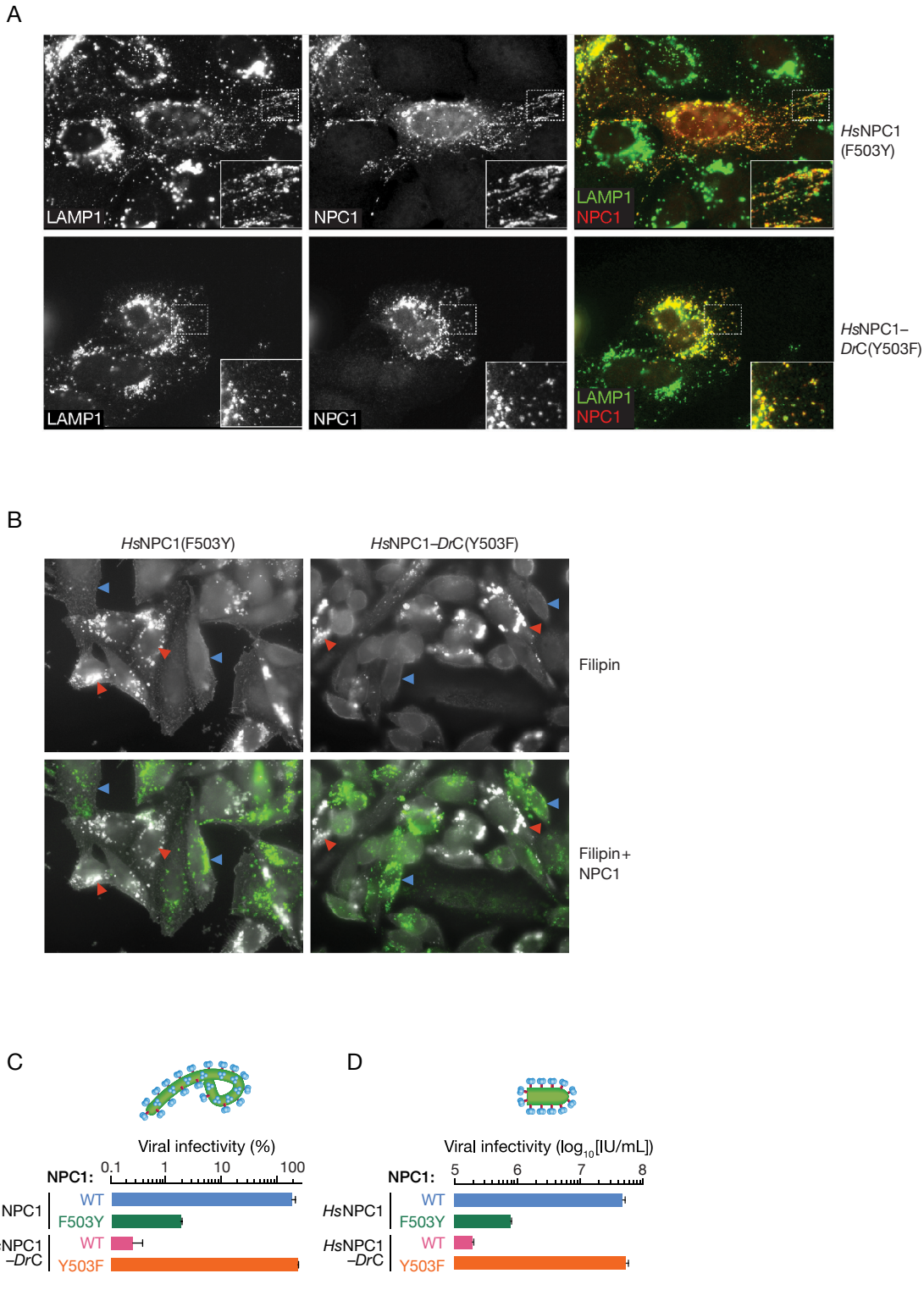

Fig 8: Residue 503 influences the capacity of full-length NPC1 to support EBOV entry and infection (A) Point mutations at residue 503 were introduced into *Hs*NPC1 and the chimera *Hs*NPC1-*Dr*C (F503Y and Y503F, respectively), and these constructs were transiently expressed in U2OS cells. NPC1 (green) and a lysosomal marker, LAMP1 (red), were visualized by immunofluorescence microscopy. (B) NPC1-deficient CHO-M12 cells stably expressing either *Hs*NPC1(F503Y) or *Hs*NPC1-*Dr*C (Y503F) were stained with filipin to visualize unesterified cholesterol. Top panel, filipin staining. Cholesterol-laden cells are marked with red arrows. Blue arrows indicate cells that are functional at cholesterol clearance. Bottom panel, cells immunostained with anti-flag antibody for NPC1 expression (green). (C) CHO-M12 cells stably expressing the NPC1 proteins indicated were exposed to authentic virus (MOI of 3), scored at 72h post infection and normalized to *Hs*NPC1 WT infectivity. (D) Infection by VSV-EBOV GP, calculated by manual counting of eGFP positive cells. IU/mL, infectious units per mL

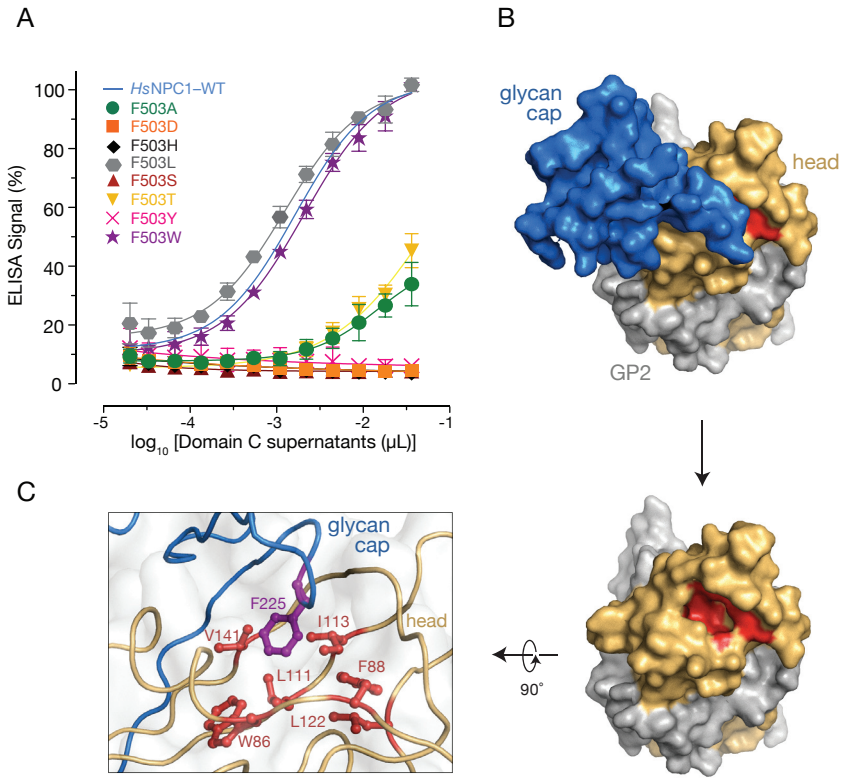

Fig 9: A bulky, hydrophobic residue is required at position 503. (A) Phe at NPC1 residue 503 was mutated to Ala, Asp, His, Leu, Ser, Thr or Trp and tested for binding to EBOV GP_{CL} by ELISA. (B) Structure of EBOV GP monomer with GP1 in orange and GP2 in grey, and glycan cap (blue) occluding the NPC1-binding site (red) (PDB ID: 3CSY [27]). Proteolytic removal of the glycan cap and mucin domain (not shown) in host cell endosomes unmasks this site. (C) Interaction between Phe 225 of the glycan cap and residues Trp86, Phe88, Leu111, Ile113, Leu122 and Val141 in the GP1 hydrophobic trough.

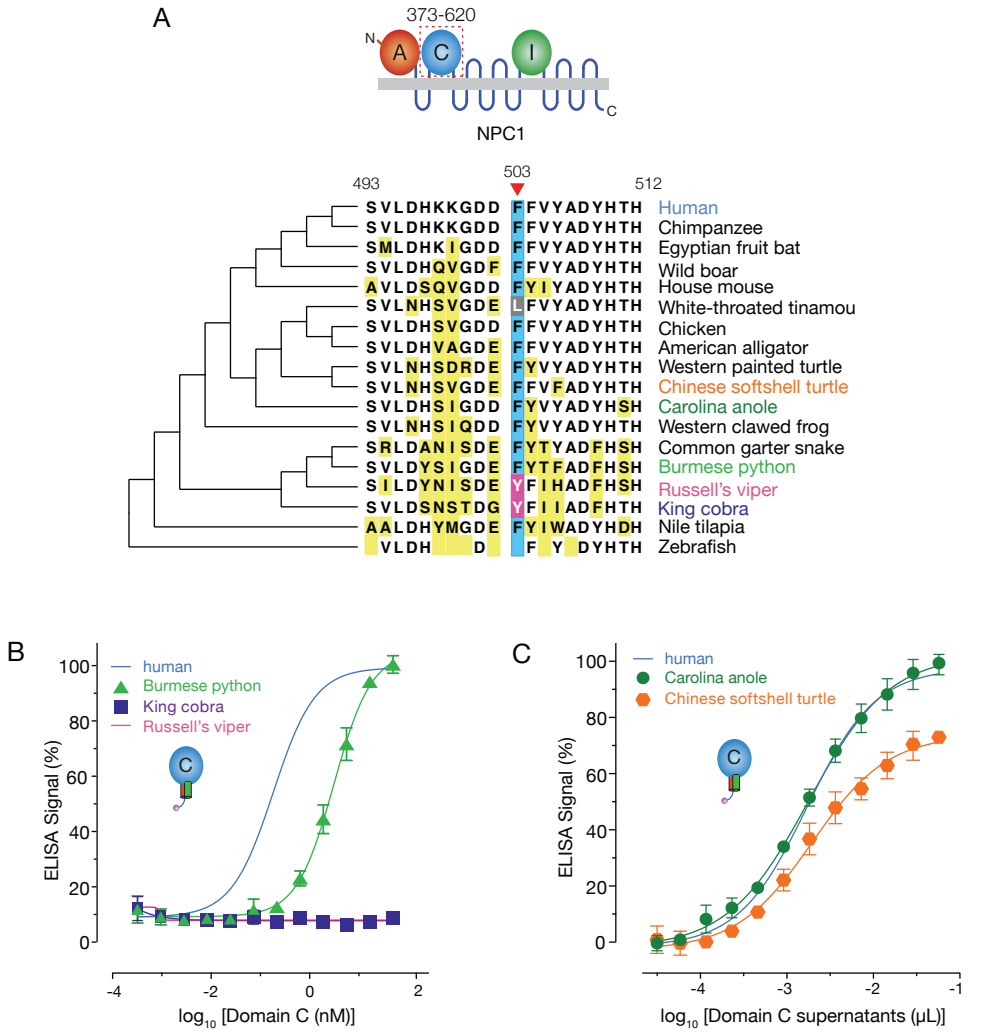

Fig 10: The Tyr residue at NPC1 position 503 is unique to the Russell's viper and king cobra NPC1 orthologs. (A) Alignment of sequences flanking residue 503 (red arrow) in domain C from divergent NPC1 orthologs. Phe 503 is shaded blue. Residues different from the human sequence are highlighted in yellow. (B) Binding of NPC1 domain C proteins from snakes (B) and other reptiles (C) to EBOV GP_{CL} was determined by ELISA.